Electronic structure study of the magnetoresistance material $CaCu_3Mn_4O_{12}$ by LSDA and LSDA+U

Hua Wu, Qing-qi Zheng, and Xin-gao Gong
Institute of Solid State Physics, Academia Sinica, P.O. Box 1129, 230031 Hefei, People's Republic of China and China Center of Advanced Science and Technology (World Laboratory), P.O. Box 8730, 100080 Beijing, People's Republic of China
(Received 24 September 1999)

The electronic structure of the large low-field magnetoresistance material $CaCu_3Mn_4O_{12}$ is calculated by using the local-spin-density approximation (LSDA) and on-site Coulomb interaction correction (LSDA+U) to the $3d$ electronic states of Cu and Mn ions. The results obtained suggest a strong ionic character of this material despite a presence of a partial Mn-O covalence effect. Three Cu ions per formula cell have their respective half-filled orbitals d_{xy}, d_{yz}, and d_{xz} due to their different local crystal environments. Four Mn ions per formula cell have nearly the same oxygen coordinations. As a consequence, the spin-up t_{2g}-like orbitals (d_{xy}, d_{yz}, and d_{xz}) are almost full-filled, while the spin-up e_g-like orbitals ($d_{3z^2-r^2}$ and $d_{x^2-y^2}$) are partially occupied due to a finite pd hybridization. And it is shown that the sublattices of Cu ions and Mn ones are both aligned in ferromagnetic order, while these two sublattices are coupled antiferromagnetically, thus giving a net spin moment of 9 μ_B per formula. The LSDA+U calculation yields a semiconducting solution, which is improved upon a half-metallic state given by the LSDA calculation and consistent with an experimental measurement.

I. INTRODUCTION

$Ln_{1-x}A_xMnO_3$ (Ln: a lanthanide, A: an alkaline-earth element) materials stimulated extensive studies because they exhibit a colossal magnetoresistance (MR) effect closely related to their structure, electronic and magnetic behaviors, and hence have a potential application to magnetic recording and sensors *et al.*[1–4] These materials have formally a mixed-valence state of $Mn^{3+}(t_{2g}^3e_g^1)$ and $Mn^{4+}(t_{2g}^3e_g^0)$. Three spin-polarized d electrons in the t_{2g} orbital of Mn^{3+} and Mn^{4+} cations form an inert spin core $S=3/2$, and the last one e_g electron is itinerant. The e_g electron transfers along the Mn^{3+}-O-Mn^{4+} route with its spin parallel to the core spin, which is responsible for both ferromagnetic (FM) order and metallic conduction of these materials, according to the double-exchange (DE) model.[5] The hopping between neighboring Mn^{3+} and Mn^{4+} cations strongly depends on the relative alignment of the Mn core spins. Consequently, the electrical resistivity is extremely sensitive to the external magnetic field. The applied magnetic field tends to align the local spins and hence leads to a rapid drop of the measured resistivity by suppressing spin fluctuations and enhancing electrical transfer, thus giving rise to the CMR effect.

The e_g orbital in the ideal perovskite $LaMnO_3$ is twofold-degenerate due to a cubic crystal field and therefore half-filled. It is well known that the Mn^{3+} cation is a Jahn-Teller (JT) ion and that the half-filled e_g state is unstable with regard to a lattice distortion, as was supported by an experimental observation that there exists a strong static JT distortion in $LaMnO_3$.[1,2] In addition, a dynamic JT effect may be important in $Ln_{1-x}A_xMnO_3$. The JT distortion results in buckling of the MnO_6 octahedral network, thereby altering the Mn-O-Mn bond angle and bond length, affecting the electron hopping probability and the DE mechanism. It was suggested that certain key aspects of CMR cannot be accounted for by DE alone, and that it seems necessary to include a striking electron-phonon coupling, which forms JT polarons and promotes charge localization against the DE process.[3,6]

It was reported very recently that perovskite-type $CaCu_3Mn_4O_{12}$ without DE exhibits large low-field MR.[7] The MR at 20 K sharply increases at low field up to -12% at 0.05 T and almost saturates at ~ 1 T. In contrast to the MR at 20 K, the MR at room temperature is almost saturated at only 0.03 T. While the common CMR materials exhibit stable and high MR only at high magnetic field up to several tesla but in a narrow temperature range. Also, at low field and room temperature, $CaCu_3Mn_4O_{12}$ exhibits a much sharper response to external magnetic field H than many other systems. In addition, the temperature stability of the MR of $CaCu_3Mn_4O_{12}$ is superior to that of $La_{0.75}Ca_{0.25}MnO_3$, a typical CMR material. Both the magnitude of low-field MR and the thermal stability of MR in $CaCu_3Mn_4O_{12}$ are shown to be of potential technological utility.[7]

$Ca^{2+}Cu_3^{2+}Mn_4^{4+}O_{12}^{2-}$ is semiconducting and orders ferromagnetically at 355 K,[7] unlike the CMR material $La_{1-x}A_xMnO_3$ ($0.2<x<0.5$) which is a FM metal. $CaCu_3Mn_4O_{12}$ has neither mixed valence of Mn cations for DE mechanism, nor the JT Mn^{3+} ions, nor a magnetically coupled metal-insulator transition,[7] as occurs in $Ln_{1-x}A_xMnO_3$ near Curie temperature. It was suggested that the MR in $CaCu_{3-x}Mn_{4+x}O_{12}$ systems is not due to the DE mechanism. Instead, the origin of the low-field MR has been interpreted in terms of tunneling MR at grain boundaries,[7] as in polycrystal samples of the perovskite manganites,[4] pyrochlore $Tl_2Mn_2O_7$[8,9] and half-metallic oxides.[10,11] In this process, the hopping of the spin-polarized electrons between

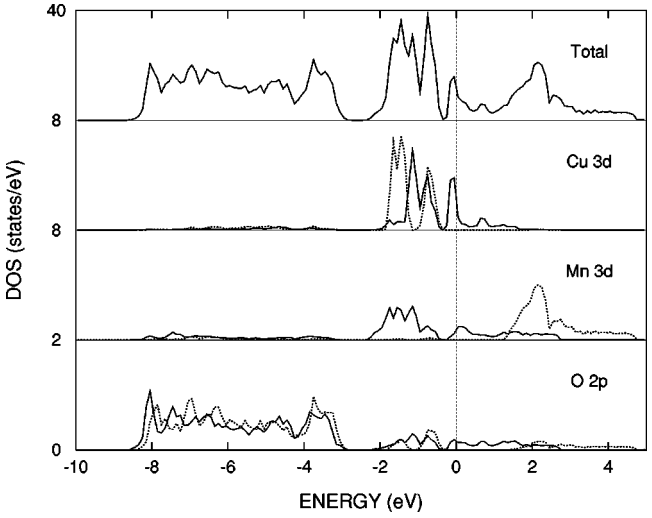

FIG. 1. Total DOS per formula and projected average DOS by LSDA. For the projected DOS, the solid (dashed) line denotes the up (down) spin, as in Figs. 2–6. Fermi level is set at the zero. A half-metallic solution is evident. See the main text for discussions.

microcrystalline grains (each with their own magnetic domains) is critically affected by a relative orientation of the magnetization, and hence may be controlled by an external magnetic field via the domain-rotation process. Thus the observed MR is due to field suppression of spin-dependent scattering at the grain or domain boundaries.[10]

$CaCu_3Mn_4O_{12}$ is a cubic perovskite-like compound with lattice constant $a=7.241$ Å.[12] Ca^{2+} and Cu^{2+} cations occupy the A sites of the ideal perovskite structure, while Mn^{4+} ions occupy the B sites. A distortion of the oxygen sublattice leads to a tilted three-dimensional network of corner-sharing MnO_6 octahedra. The Mn-O-Mn bond angle is 142° instead of 180° in the ideal perovskite structure. Reference 12 can be referred to, regarding the detailed data of the crystal structure (see Fig. 1 and Tables II and IV in Ref. 12).

It is intended in this work to study the electronic structure of this new-type MR material by the first-principle calculations within the LSDA (Ref. 13) and LSDA+U (Ref. 14) formalisms. The linear combination of atomic orbitals (LCAO) band method[15] is adopted, which has been applied to electronic-structure calculations for some materials.[16,17] Quasi-self-consistent ionic basis functions are generated by solving Hohenberg-Kohn-Sham equation[13] iteratively for an individual atom in the crystal environment, and Ca $4s$, Cu $3d4s$, Mn $3d4s$, and O $2s2p$ orbitals are chosen as the valence states. Hartree potential is expanded into lattice harmonics up to $L=4$, and exchange-correlation potential of von Barth–Hedin type[18] is used.

First, we calculate the electronic structure within LSDA, which shows to be a half-metallic narrow band structure. Next, we argue that $CaCu_3Mn_4O_{12}$ is a strongly correlated electron system like common transition-metal oxides, and hence we employ the so-called LSDA+U method where the strong d-d electron correlations are incorporated into the LSDA scheme. As will be seen below, the LSDA+U calculation gives a semiconducting solution, which is improved on the LSDA result of half-metallicity and consistent with the experimental measurement.

II. RESULTS AND DISCUSSIONS

The LSDA results are shown in Figs. 1–3 for total and projected density of states (DOS). The LSDA solution appears half-metallic–metallic for spin-up electrons while insulating for spin-down electrons. In this case, the conducting electrons are fully spin-polarized. Such an effect was first discussed for the alloy NiMnSb, which was theoretically predicted and then experimentally confirmed to be a half-metallic ferromagnet.[19] Half-metallicity was recently applied to an account of enhanced spin-dependent magnetotransport behavior of MR materials such as $La_{1-x}Ca_xMnO_3$ ($0.2<x<0.5$),[1] double-perovskite Sr_2FeMoO_6,[10] and CrO_2 films.[11] Also, various attempts have been made to seek for this new class of half-metallic materials due to their potential applications to ''spin-electron'' devices.[20,21]

As seen in Fig. 1, Cu $3d$ bands mostly lie between binding energy $E_b=2$ eV and Fermi level E_F. The spin-down Cu $3d$ states are full-filled, while the spin-up Cu $3d$ states are partial-filled (and contribute a little to the DOS at E_F), giving a minus spin moment of $-0.71\ \mu_B$ per Cu ion. For an explicit view, also we plot the DOS projected onto five Cu $3d$ orbitals, as seen in Fig. 2. Owing to the different spatial configurations of coordinated oxygens (see Fig. 1 in Ref. 12), three Cu ions per formula cell exhibit different orbital occupancies. For the Cu ion at the site (0.5,0,0), the d_{xy} orbital is coupled to the O $2p$ orbitals along the b-axis direction and hence forms a relatively dispersive band [see Fig. 2(a)]. The spin-down d_{xy} orbital is full-filled due to a large spin-splitting of 1.5 eV, while the spin-up d_{xy} orbital is nearly empty. And other four d orbitals are almost full-filled with a small spin-splitting of 0.6 eV, except that the spin-up e_g-like orbitals ($3z^2$-r^2 and x^2-y^2) contribute a little to the narrow bands across E_F. Similarly, the $3d$ orbitals of the Cu ion at (0,0.5,0) are almost full-filled except for the half-filled d_{yz} orbital with a nearly full spin polarization, as shown in Fig. 2(b). While only the d_{xz} orbital is half-filled for the Cu ion at (0,0,0.5), as seen in Fig. 2(c).

In contrast, the $3d$ states of four Mn cations per formula cell are similar to each other due to their similar oxygen environments.[12] Therefore, we plot the projected DOS for the $3d$ orbitals of only the Mn ion at (0.25,0.25,0.25), as seen in Fig. 3. It is evident that the t_{2g}-like orbitals (xz, yz and xy) are almost half-filled and fully spin-polarized with the same spin splitting of 3.5 eV, and that the spin-up e_g-like orbitals are slightly occupied due to a finite Mn $3d$-O $2p$ hybridization effect. As a result of spin dependence of the Mn $3d$-O $2p$ hybridization, the spin-up channel is conducting while the spin-down one is insulating.

In addition, the O $2p$ states of the oxygen anions mostly distribute over the energy range from $E_b=3$ to 8 eV (see the lowest panel of Fig. 1), where minor Cu $3d$ and Mn $3d$ states are mixed also due to the pd hybridizations. And a small component of the O $2p$ states lies in the energy region of the Cu $3d$ and Mn $3d$ states discussed above. Whereas the empty $4s$ states of Ca, Cu, and Mn cations lie mostly above E_F by 5, 7, and 12 eV, despite their distribution over a wide energy range. Thus, the Ca atoms denote their $4s$ electrons to the active Mn-O bands, and no Ca $4s$ electrons contribute to the transport properties, as the Tl $6s$ electrons in $Tl_2Mn_2O_7$ where an itinerant Tl-O-Mn hybridized state is

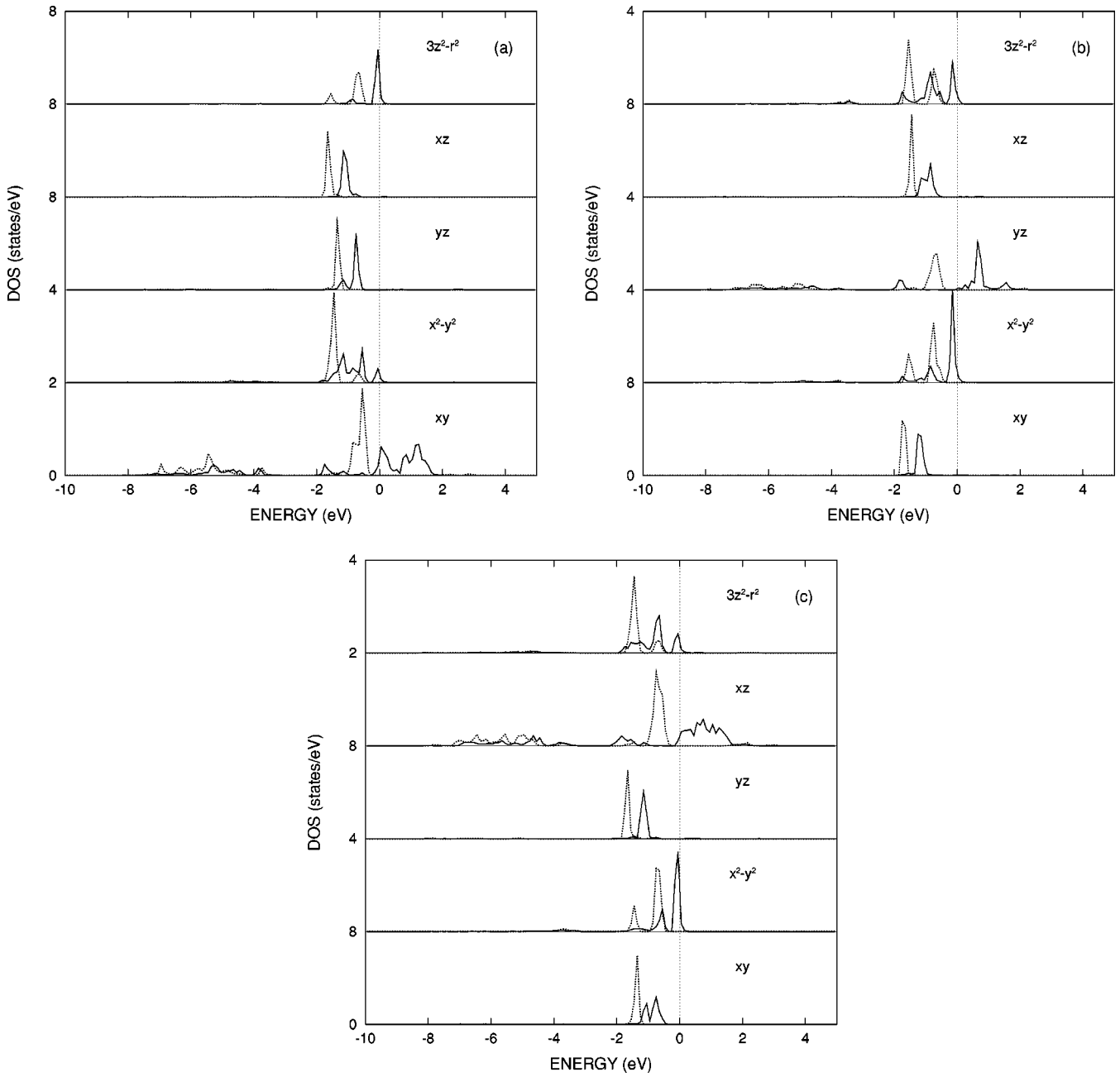

FIG. 2. Projected DOS by LSDA for the $3d$ orbitals of the Cu cations at different sites (a) (0.5,0,0), (b) (0,0.5,0), and (c) (0,0,0.5). The d_{xy}, d_{yz}, and d_{xz} orbitals are in turn nearly half-filled.

formed in part due to the short bond length.[8,22]

The present results support a proposal of a strong ionic character for $CaCu_3Mn_4O_{12}$, despite that the Mn cation deviates a little from the formal tetravalence due to a partial pd covalence effect, as is the case for many ionic oxides.[1,15,16] This point could be inferred from the fact that the Mn-O bond length of 1.915 Å is smaller than a sum ($\approx$2.1 Å) of two corresponding ionic radii ($R_{Mn^{4+}} \approx 0.7$ Å, $R_{O^{2-}} \approx 1.4$ Å), while three sets of Cu-O distances of 1.942, 2.707, and 3.181 Å are close to or much larger than the corresponding sum approximately equal to 2.1 Å ($R_{Cu^{2+}} \approx 0.7$ Å).[12] Naturally, there exists a little stronger covalence effect in the Mn-O bonds than in the Cu-O bonds.

It is shown above that the spin moment of the Cu cations ($-0.71\ \mu_B$) is carried mostly by one of the t_{2g}-like orbitals (xz,yz, and xy), respectively. Next, the Mn cation has the same spin moment of $3\ \mu_B$ as expected for the formally Mn^{4+} cation with a spin $S=3/2$, and the moment is carried mainly by the t_{2g} orbitals ($2.3\ \mu_B$) and a little by the e_g orbitals ($0.7\ \mu_B$). In addition, the present calculation indicates a small but nonvanishing spin moment of $-0.08\ \mu_B$ carried by the O anions, as in the case of the perovskite $LaMnO_3$ (Ref. 1) and pyrochlore $Tl_2Mn_2O_7$.[22] The present results suggest that the Cu and Mn sublattices are both aligned ferromagnetically, while both of the sublattices are coupled antiferromagnetically. A similar case occurs in the double-perovskite MR material Sr_2FeMoO_6, where exists an antiferromagnetic coupling between the Fe and Mo sublattices.[10] Consequently, this ferrimagnetic state of $CaCu_3Mn_4O_{12}$ gives a net spin moment of $9\ \mu_B$ per formula,

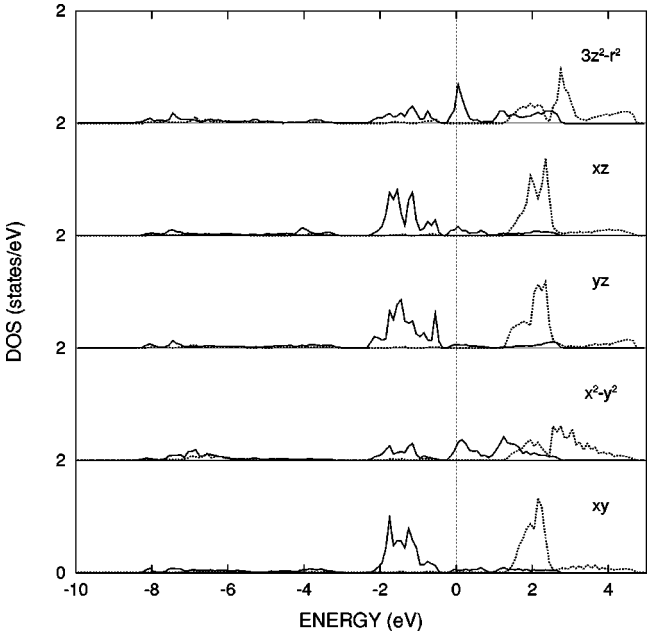

FIG. 3. Projected DOS by LSDA for the Mn $3d$ orbitals. The t_{2g}-like orbitals are nearly half-filled, while the e_g-like orbitals are a little occupied due to pd hybridizations.

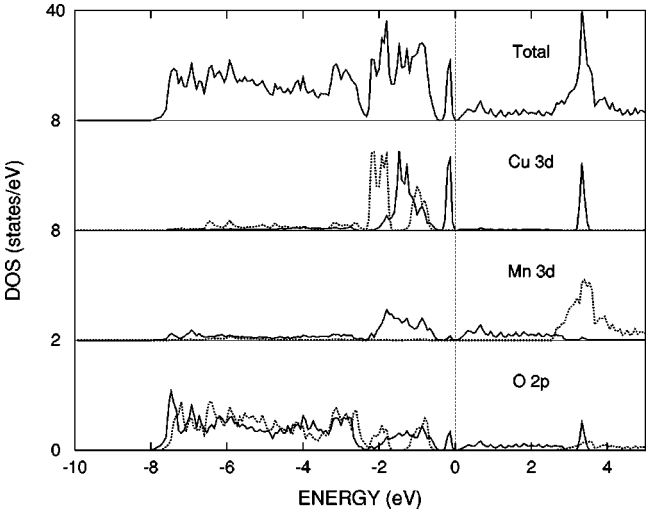

FIG. 4. Total DOS per formula and projected average DOS for a semiconducting solution by LSDA+U. The Cu $3d$ and Mn $3d$ states are modified remarkably due to on-site Coulomb interactions.

which is consistent with a prediction from an ionic model but a little larger than an experimental value of 7 μ_B (Ref. 23) derived from a magnetization measurement. This discrepancy could be due to impurity effects or defect ones, both of which would reduce the ordered spin moment.[8,10]

It can be seen in Figs. 1–3 that $CaCu_3Mn_4O_{12}$ has a narrow band structure like the common transition-metal oxides. The narrow-band behavior implies strong localization of electrons in materials, which leads to strong on-site Coulomb interactions and hence results in a redistribution of electronic states.[2] In view of the fact that LSDA, something like a mean-field method with an underestimation of electronic correlations, usually fails to give a satisfactory description for strongly correlated electron systems,[2,14–17] we also include the on-site Coulomb interaction correction and adopt the so-called LSDA+U scheme to further our calculation.

The U-corrected potential dependent on m orbital and σ spin of the Cu $3d$ and Mn $3d$ states is expressed as follows:

$$V_{m\sigma}^{\mathrm{LSDA+U}} = V^{\mathrm{LSDA}} + U\sum_{m'} (n_{m'-\sigma} - n^0) + U \sum_{m'(\neq m)} (n_{m'\sigma} - n^0) - J \sum_{m'(\neq m)} (n_{m'\sigma} - n_\sigma^0),$$

which includes the effects of Hubbard U term in a mean-field sense.[24] The last term (J is an intraatomic exchange parameter) is subtracted from the expression above in order to avoid double counting of the interactions. Owing to a presence of screening effects and interorbital hybridizations, it is hard to evaluate accurately the U and J in solids. A common ''constraint'' density-functional calculation usually gives a somewhat overestimated U due to an underestimation and even negligence of the screening and hybridization effects.[14] Thus U and J are estimated or empirically chosen in many cases. In a recent reformulation of the LDA+U method for a local orbital basis, it was proposed that the values of U are typically only 40–60% as large as values currently in use.[25] This suggestion is consistent with the work in Ref. 26, and some of the former values of U proved appropriate in our recent works.[16,17]

In general, U increases gradually while J varies slightly from early transition-metal oxides to late transition-metal ones.[14] It can be seen from the results above that the Mn $3d$ states are less localized than the Cu $3d$ states. In particular, the Mn e_g-like orbitals are more delocalized than the Mn t_{2g}-like ones due to the stronger $pd\sigma$-type hybridization for the former than the $pd\pi$-type one for the latter. As a result, the U interactions on the Mn sites are partially screened by the delocalized e_g electrons. The role of the e_g screening in $LaMO_3$ (M:Ti-Cu) perovskites was discussed in detail in Ref. 27, where the effective Coulomb interactions were estimated. Specifically, the decreasing $U \sim 2$ eV was evaluated for the Mn $3d$ electrons in $LaMnO_3$.[27] Similarly, we choose $U=2$ eV for the Mn $3d$ electrons in $CaCu_3Mn_4O_{12}$, and a larger $U=5$ eV for the Cu $3d$ electrons as in the case of other cuprates,[17] as well as the same $J=1$ eV for both the Cu $3d$ and Mn $3d$ electrons.[27] Although the LSDA+U result is not a substitute for a true many-body solution, it does provide important guidelines, as will be seen below.

The LSDA+U calculation yields a semiconducting solution (with a minor gap lying between the spin-up Cu $3d$ and Mn $3d$ bands), which is consistent with an experimental measurement.[7] A comparison between Fig. 1 and Fig. 4 suggests that the Cu $3d$ and Mn $3d$ states are modified remarkably by the U interactions. For example, the projected $3d$ DOS given by LSDA+U for the Cu cation at (0.5,0,0) is plotted in Fig. 5. In particular, the empty spin-up d_{xy} band shifts up to 3.3 eV above E_F due to the strong on-site Coulomb repulsions, and this band becomes even more narrow due to a subsequent enhanced orbital polarization. On the other hand, the other Cu $3d$ bands move downward by a little, and thus the $3d$ bands derived from the e_g-like orbitals do not cross E_F and become full-filled. Meanwhile, the spin-down Mn t_{2g} bands move up by $\sim$1.2 eV, while the Mn e_g bands undergo fewer changes due to a little stronger pd hy-

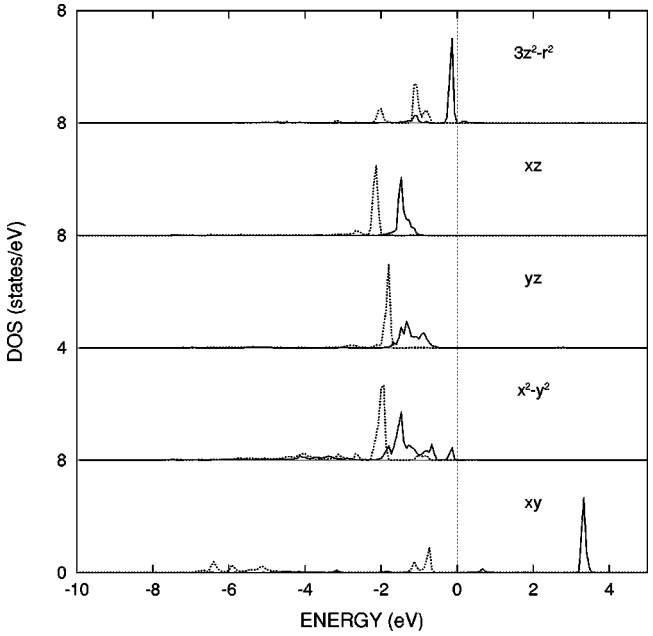

FIG. 5. Projected DOS by LSDA+U for the 3*d* orbitals of the Cu cation at (0.5,0,0).

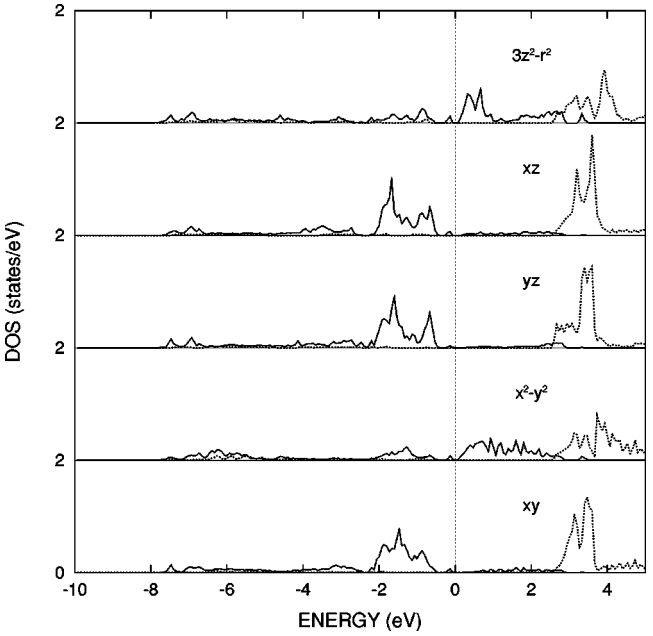

FIG. 6. Projected DOS by LSDA+U for the Mn 3*d* orbitals.

bridization against the on-site U interactions, as seen in Fig. 6. As a striking feature, a semiconducting gap is present in this LSDA+U solution.

The calculated ionic valences remain almost unchanged, whereas the assignment of charge and spin to the different orbitals undergoes little change due to the enhanced orbital- and spin-polarizations induced by the U interactions. The local spin moment of Cu, Mn and O ions increases up to -0.83, 3.17, and $-0.1\ \mu_B$, respectively, thus giving the same total spin moment of 9 μ_B per formula as the LSDA result above.

For the group of Cu 3*d* bands, there exists a large insulating gap of ~ 3.5 eV, as seen in Fig. 5. Also, the bandwidth is less than 1 eV, e.g., only ~ 0.2 eV for the topmost $d_{3z^2-r^2}$ valence band. Both indicate that the Cu 3*d* electrons are highly localized and the Cu cations keep their intraatomic behavior. It is suggested that the Cu 3*d* electrons may contribute less to the transport property of $CaCu_3Mn_4O_{12}$. On the other hand, although there is a small charge occupancy over the Mn e_g orbitals as a result of a finite pd covalence effect, the e_g electrons are not itinerant due to the presence of a semiconducting gap. Thus, the DE mechanism could be precluded from the origins of the MR effect in $CaCu_3Mn_4O_{12}$. Instead, an intergrain-interdomain tunneling mechanism[4,9–11] was proposed to be an origin of the MR behavior.[7] This proposal was supported by experimental measurements that the magnitude of the saturated magnetic field in the FM-domain reorientation (the coercive field) is nearly the same as that in the observed MR, and that the MR magnitude would be scaled by a square of the magnetization order parameter.[7] The latter result is in accord with a consequence of the mechanism that the spin-dependent scattering at the magnetic domain boundaries is totally responsible for the observed MR.[4,10]

ACKNOWLEDGMENTS

This work was supported by the PanDeng Project (95-Yu-41) and NSF of China (19574057), and it was financed by CAS (LWTZ-1298).

[1] W.E. Pickett and D.J. Singh, Phys. Rev. B **53**, 1146 (1996).
[2] S. Satpathy, Z.S. Popovic, and F.R. Vukajlovic, Phys. Rev. Lett. **76**, 960 (1996).
[3] K. Liu, X.W. Wu, K.H. Ahn, T. Sulchek, C.L. Chien, and J.Q. Xiao, Phys. Rev. B **54**, 3007 (1996).
[4] H.Y. Hwang, S.-W. Cheong, N.P. Ong, and B. Batlogg, Phys. Rev. Lett. **77**, 2041 (1996).
[5] C. Zener, Phys. Rev. **82**, 403 (1951).
[6] A.J. Millis, P.B. Littlewood, and B.I. Shraiman, Phys. Rev. Lett. **74**, 5144 (1995).
[7] Z. Zeng, M. Greenblatt, M.A. Subramanian, and M. Croft, Phys. Rev. Lett. **82**, 3164 (1999).
[8] Y. Shimakawa, Y. Kubo, and T. Manako, Nature (London) **379**, 53 (1996).
[9] H.Y. Hwang and S.-W. Cheong, Nature (London) **389**, 942 (1997).
[10] K.-L. Kobayashi, T. Kimura, H. Sawada, K. Terakura, and Y. Tokura, Nature (London) **395**, 677 (1998).
[11] H.Y. Hwang and S.-W. Cheong, Science **278**, 1607 (1997).
[12] J. Chenavas, J.C. Joubert, M. Marezio, and B. Bochu, J. Solid State Chem. **14**, 25 (1975).
[13] P. Hohenberg and W. Kohn, Phys. Rev. **136**, B864 (1964); W. Kohn and L.J. Sham, Phys. Rev. **140**, A1133 (1965).
[14] V.I. Anisimov, J. Zaanen, and O.K. Andersen, Phys. Rev. B **44**, 943 (1991).
[15] H. Wu, M.C. Qian, and Q.Q. Zheng, J. Phys.: Condens. Matter **11**, 209 (1999).
[16] H. Wu and Q.Q. Zheng, Phys. Rev. B **59**, 15 027 (1999).

[17] H. Wu, Q.Q. Zheng, X.G. Gong, and H.Q. Lin, J. Phys.: Condens. Matter **11**, 4637 (1999).
[18] U. von Barth and L. Hedin, J. Phys. C **5**, 1629 (1972).
[19] R.A. de Groot, F.M. Mueller, P.G. van Engen, and K.H.J. Buschow, Phys. Rev. Lett. **50**, 2024 (1983).
[20] H. van Leuken and R.A. de Groot, Phys. Rev. Lett. **74**, 1171 (1995).
[21] W.E. Pickett, Phys. Rev. B **57**, 10 613 (1998).
[22] D.J. Singh, Phys. Rev. B **55**, 313 (1997).
[23] It can be seen from the top panel of Fig. 3 in Ref. 7 that the saturated magnetization of $CaCu_3Mn_4O_{12}$ at 20 K is nearly 4×10^4 emu/mole. Thus, an experimental value of $7\mu_B$ for the magnetic moment per formula can be estimated from the calculation $(4\times10^4\text{emu}/6.02\times10^{23})/(0.927\times10^{-20}\text{emu}/1\mu_B) = 7.17\ \mu_B$.
[24] Pan Wei and Zheng Qing Qi, Phys. Rev. B **49**, 10 864 (1994); **49**, 12 159 (1994).
[25] W.E. Pickett, S.C. Erwin, and E.C. Ethridge, Phys. Rev. B **58**, 1201 (1998).
[26] J. Hugel and M. Kamal, Solid State Commun. **100**, 457 (1996).
[27] I. Solovyev, N. Hamada, and K. Terakura, Phys. Rev. B **53**, 7158 (1996).